



HAL
open science

Mixed Valence Tungsten (IV,V) Compounds with Layered Structures (Part III*): Synthesis and Crystal Structure of $\text{Ag}_{1-x}[\text{W}_2\text{O}_2\text{Cl}_6]$ and Investigations on the Ag^+ Ion Mobility

Johannes Beck, Wilfried Hoffbauer, Christian Kusterer, Marcel Schieweling

► **To cite this version:**

Johannes Beck, Wilfried Hoffbauer, Christian Kusterer, Marcel Schieweling. Mixed Valence Tungsten (IV,V) Compounds with Layered Structures (Part III*): Synthesis and Crystal Structure of $\text{Ag}_{1-x}[\text{W}_2\text{O}_2\text{Cl}_6]$ and Investigations on the Ag^+ Ion Mobility. *Journal of Inorganic and General Chemistry / Zeitschrift für anorganische und allgemeine Chemie*, 2010, 636 (9-10), pp.1827. 10.1002/zaac.201000080 . hal-00552461

HAL Id: hal-00552461

<https://hal.science/hal-00552461>

Submitted on 6 Jan 2011

HAL is a multi-disciplinary open access archive for the deposit and dissemination of scientific research documents, whether they are published or not. The documents may come from teaching and research institutions in France or abroad, or from public or private research centers.

L'archive ouverte pluridisciplinaire **HAL**, est destinée au dépôt et à la diffusion de documents scientifiques de niveau recherche, publiés ou non, émanant des établissements d'enseignement et de recherche français ou étrangers, des laboratoires publics ou privés.



**Mixed Valence Tungsten (IV,V) Compounds with Layered
Structures (Part III*): Synthesis and Crystal Structure of
Ag_{1-x}[W₂O₂Cl₆] and Investigations on the Ag⁺ Ion
Mobility**

Journal:	<i>Zeitschrift für Anorganische und Allgemeine Chemie</i>
Manuscript ID:	zaac.201000080
Wiley - Manuscript type:	Article
Date Submitted by the Author:	07-Feb-2010
Complete List of Authors:	Beck, Johannes; University of Bonn, Inorganic Chemistry Hoffbauer, Wilfried Kusterer, Christian Schieweling, Marcel
Keywords:	Halooxotungstates, Mixed valence compounds, Ion mobility, 109Ag solid state NMR, Small Gap Semiconductivity



1
2
3
4 **Mixed Valence Tungsten (IV,V) Compounds with Layered**
5 **Structures (Part III*): Synthesis and Crystal Structure of**
6 **Ag_{1-x}[W₂O₂Cl₆] and Investigations on the Ag⁺ Ion Mobility**
7
8
9

10
11
12
13
14
15 **Johannes Beck****, Wilfried Hoffbauer, Christian Kusterer and Marcel Schieweling

16 Bonn, Institut für Anorganische Chemie der Universität
17
18
19
20
21
22
23
24

25 Received.....
26
27
28
29
30
31
32
33

34 Dedicated to Prof. Bernd Harbrecht on the Occasion of his 60th Birthday
35
36
37
38
39
40
41
42
43
44
45
46
47

48 _____
49 * Second Report: see ref. [2]
50
51

52 **Prof. Dr. J. Beck

53 Inst. f. Anorg. Chemie d. Universität

54 Gerhard-Domagk-Str. 1

55 D-53121 Bonn

56 e-mail: j.beck@uni-bonn.de
57
58
59
60

1
2
3 **Abstract.** The reactions of metallic silver with tungsten tetrachlorideoxide WOCl_4 or the reaction of
4 AgCl with WOCl_3 , both at 690 K, lead to $\text{Ag}_{1-x}[\text{W}_2\text{O}_2\text{Cl}_6]$ as black lustrous crystal needles. The
5 compound shows a substantial phase field width in the silver content depending on reaction tem-
6 perature and reaction time and crystals with $x = 0, 0.38$ and 0.82 were isolated. The crystal structure
7 determinations (monoclinic, $C2/m$) show the structure to be isotopic to those of $\text{Tl}[\text{W}_2\text{O}_2\text{Cl}_6]$ and
8 $\text{K}_{0.84}[\text{W}_2\text{O}_2\text{Cl}_6]$ with the presence of 1-D polymeric $[\text{W}_2\text{O}_2\text{Cl}_6]_n$ strands and Ag^+ ions with a variety
9 in the occupation of the respective crystallographic site. $\text{Ag}_{1-x}[\text{W}_2\text{O}_2\text{Cl}_6]$ represents a mixed valence
10 compound with a variable ratio of W(IV) and W(V) in the W_2 dumbbells with a short W–W separa-
11 tion of 2.85 Å. In Fourier maps the electron density of the Ag ion appears smeared over a large area.
12 By structure determinations of stoichiometric $\text{Ag}_{1.0}[\text{W}_2\text{O}_2\text{Cl}_6]$ at temperatures of 123, 193, and 293
13 K a double minimum potential was found with the silver ion dynamically disordered over two flat
14 basins with a thermal activation barrier of 13 meV. No long range ion mobility is present since the
15 Ag^+ ions are trapped within a coordinating cage consisting of ten Cl atoms of the surrounding
16 $[\text{W}_2\text{O}_2\text{Cl}_6]$ strands forming a distorted bicapped cube. By MAS-NMR measurements on the ^{109}Ag
17 nuclei at different temperature the spin lattice relaxation times were determined giving a thermally
18 activated barrier of 15 meV. The electronic conductivity of pressed powder samples of
19 $\text{Ag}[\text{W}_2\text{O}_2\text{Cl}_6]$ by a four-probe measurement applying direct current is $1 \Omega^{-1} \text{cm}^{-1}$ at room tempera-
20 ture and $10^{-3} \Omega^{-1} \text{cm}^{-1}$ at 25 K. For the conduction mechanism at low temperatures a *variable range*
21 *hopping* mechanism is suggested while at higher temperatures a standard semi-conductivity with a
22 band gap of 60 meV is present.
23
24
25
26
27
28
29
30
31
32
33
34
35
36
37
38
39
40
41
42
43
44
45
46
47
48

49 **Keywords:** Halooxotungstates; Mixed valence compounds; Nonstoichiometry; Ion mobility; ^{109}Ag
50 solid state NMR; Small Gap Semiconductivity
51
52
53
54
55
56
57
58
59
60

Introduction

In preceding works we reported on the structure of WOCl_3 and the structures and properties of the chlorooxotungstates $M_x[\text{W}_2\text{O}_2\text{Cl}_6]$ with $M = \text{Tl}^+, \text{K}^+, \text{Pb}^{2+}, \text{Hg}^{2+}$ and the non-stoichiometric phases $\text{Ag}_{0.8}[\text{W}_2\text{O}_2\text{Br}_6]$ [1], $\text{Cu}_{1-x}[\text{W}_2\text{O}_2\text{Cl}_6]$ and $\text{Cu}_{1-x}[\text{W}_4\text{O}_4\text{Cl}_{10}]$ [2]. All compounds represent a family of mixed valence compounds with structures build of negatively charged infinite $\text{W}_2\text{O}_2\text{X}_6$ double strands consisting of WO_2X_4 octahedra condensed via two edge-sharing halogen atoms to form double octahedra and corner-sharing oxygen atoms to build 1-D strands. The mono or divalent cations are located between the strands and connect them to layers. The first representatives of this structure type were the bromooxotungstates $\text{Na}[\text{W}_2\text{O}_2\text{Br}_6]$ [3] and the non-stoichiometric $\text{Ag}_{0.74}[\text{W}_2\text{O}_2\text{Br}_6]$ [4]. The structures of these compounds can in principle be understood as intercalates with WOX_3 ($X = \text{Cl}, \text{Br}$) acting as the host for atoms of the corresponding metals or, in the case of $\text{Cu}_{1-x}[\text{W}_4\text{O}_4\text{Cl}_{10}]$, as intermediates between WOX_3 and WOX_2 . The tungsten(IV) dihalideoxides crystallize most probably isotypic to the structure of MoOCl_2 which has been investigated by *Thiele* et al. [5,6] despite the structure of WOCl_2 is not known in detail. WOCl_2 is a product of thermal decomposition of WOCl_3 .

Several of the compounds investigated so far show non-stoichiometric compositions with a phase field width pertaining the cations M , which are observed to underoccupy their positions. The compounds have been found to be weakly paramagnetic with temperature independent Pauli characteristics and show a remarkably high electrical conductivity of about $0.1 \Omega^{-1} \text{cm}^{-1}$ or higher at room temperature. The temperature dependence of the conductivity corresponds to semiconducting behaviour with a very small thermal activation barrier for the conduction process of about 0.03 eV at room temperature. The physical properties of the compounds can be understood by an interpretation as being one-dimensional metals. The real structure of the crystals, however, with a high number of discontinuances of the one-dimensional building units, limits the conductivity in close analogy to Krogmann's salts [7].

Here we report on $\text{Ag}_{1-x}[\text{W}_2\text{O}_2\text{Cl}_6]$ as the silver containing representative of the $(M^+)_x[\text{W}_2\text{O}_2\text{Cl}_6]$ family of compounds and its remarkable properties.

Experimental

All educts and reaction products were handled in an argon filled glove box. Ampoules were made of borosilicate glass and flame-dried in vacuo prior to use. WOCl_4 was prepared from freshly precipitated WO_3 , which was obtained from a NaWO_4 solution (Merck) by precipitation with concentrated hydrochloric acid. WO_3 was refluxed in SOCl_2 (Merck) and the orange solid was isolated by

1
2
3 filtration under argon. Before use, WOCl_4 was sublimated twice [8]. WOCl_3 was prepared by reduc-
4 tion of WOCl_4 with Al powder in evacuated borosilicate glass tubes at 500 K. AlCl_3 formed in the
5 reaction was sublimated to the cold tip of the ampoule before opening in the glove box. AgCl was
6 freshly prepared by precipitation from AgNO_3 and hydrochloric acid. It was handled in the dark and
7 dried over P_4O_{10} .
8
9

10 11 12 13 *Synthesis*

14 $\text{Ag}_{1-x}[\text{W}_2\text{O}_2\text{Cl}_6]$ was prepared by two ways, either by the reduction of WOCl_4 with metallic silver
15 (Method A) or by reaction of WOCl_3 with AgCl (Method B), respectively.
16
17
18
19

20
21 *Method A:* For the reduction of WOCl_4 with Ag 1965 mg WOCl_4 (5.752 mmol) and 463 mg Ag
22 powder (4.292 mmol) were filled into an ampoule of 15 cm length an 1.8 cm diameter, which was
23 sealed, placed in a horizontal tube furnace and heated to a temperature of 690 K for a period of 7
24 days. The product was obtained as black needles with metallic luster. The crystals were separated
25 manually for crystal structure analysis and solid state NMR investigations.
26
27
28
29
30

31
32 *Method B:* For the reaction of WOCl_3 with silver chloride 136 mg WOCl_3 (0.45 mmol) and 70 mg
33 AgCl (0.49 mmol, dried in vacuo) and were filled together with a small amount (32 mg) WCl_6
34 (0.08 mmol) into an ampoule of 13 cm length and 6 mm diameter. This ampoule was placed in a
35 horizontal tube furnace and heated starting from 510 K up to 700 K during a period of 40 days.
36 Along the ampoule a temperature gradient of 20 K was present with the starting materials posi-
37 tioned in the hotter zone. At a temperature of 620 K crystallization of black needles started. The
38 crystals grew on the surface of the sintered starting materials, chemical transport could not be ob-
39 served. Crystals were separated manually and the residual ampoule content was grinded and sealed
40 once more in an evacuated ampoule for further reaction at 690 K. A second crop of crystals could
41 be separated manually.
42
43
44
45
46
47
48
49
50

51 52 *Crystal structure determinations*

53
54 Crystals from different synthetic runs were mounted in thin-walled glass capillaries, which were
55 sealed. Data were collected using a Enraf-Nonius-Kappa-CCD diffractometer using graphite mono-
56 chromatized Mo- $K\alpha$ radiation. Low temperature was maintained with a nitrogen gas flow cooling
57 system (Oxford Cryosystems). Temperatures were calibrated with a micro-thermocouple mounted
58 in the position of a crystal. Data sets were recorded at ambient temperature and additionally at
59
60

1
2
3 193 K and 123 K. Due to the high absorption coefficients and the anisotropic shape of the crystals a
4 numerical absorption correction with the aid of the program HABITUS [10] was applied to all data
5 sets. The optimization of the crystal shape was performed by minimization of the reliability factor
6 of averaging symmetry equivalent reflections. Structure models were obtained by direct methods
7 and refined against F^2 using SHELX97 [11] as implemented in the WINGX program package [12].
8 Tab. 1 contains the crystallographic data and details of the structure analyses, positional parameters
9 are given in Table 2. Additionally, the crystal structures were refined against F^2 using the program
10 JANA2000 [13] and the Gram-Charlier expansion to calculate anharmonic displacement tensors.
11
12
13
14
15
16
17
18

19 Further details of the crystal structure investigations have been deposited and may be obtained from
20 the Fachinformationszentrum Karlsruhe, D-76344 Eggenstein-Leopoldshafen, Germany (e-mail:
21 crysdata@fiz-karlsruhe.de), on quoting the deposition numbers CSD-421449 (293 K), CSD-421448
22 (193 K) and CSD-421447 (123 K) for $\text{Ag}[\text{W}_2\text{O}_2\text{Cl}_6]$.
23
24
25
26
27

28 *Nuclear magnetic resonance analysis*

29
30 An amount of selected crystals obtained by method A was grinded and filled into a rotor and sealed
31 by a vespel cap. The rotor was placed inside a 4 mm MAS probe (Chemagnetics) allowing for a
32 maximum spinning rate of 18 kHz in the temperature range from 120 to 520 K. Data were collected
33 with a 400 MHz spectrometer (Varian Infinity+). A 9 mol L^{-1} AgNO_3 solution spiked with
34 0.25 mol L^{-1} $\text{Fe}(\text{NO}_3)_3$ for acceleration of the relaxation process was used as reference.
35
36
37
38
39
40

41 *Conductivity Measurements*

42
43 A sample of $\text{Ag}[\text{W}_2\text{O}_2\text{Cl}_6]$, prepared via method B, was grinded and pressed to a pellet of 6 mm
44 diameter. The bulk sample was checked by X-ray powder diffractometry and EDX analysis for pu-
45 rity. Only marginal reflections of AgCl were present with a maximal relative intensity of 1 %. The
46 silver content was found to be stoichiometric by EDX. Conductivity measurements were performed
47 by four-probe technique applying direct current within the temperature range from 10 K to 300 K,
48 in both directions with cooling and heating.
49
50
51
52
53
54
55
56
57
58
59
60

Results and Discussion

Synthesis

The silver oxochlorotungstate $\text{Ag}[\text{W}_2\text{O}_2\text{Cl}_6]$ can be obtained by two different methods. In the presence of AgCl thermal decomposition of WOCl_3 occurs according to Eq. (A).



Metallic silver reduces WOCl_4 according to Eq. (B) under formation of AgCl.



While reaction A gives the product in higher purity, reaction B gives a higher yield according to the higher reactivity of WOCl_4 . The higher purity in reaction A is a consequence of the high volatility of WOCl_4 , which can be sublimated off from the product whereas AgCl as the side-product of reaction B is not volatile. Additionally, the thermal decomposition of WOCl_3 to WOCl_2 and WOCl_4 at the applied temperatures is a distracting rival to the desired reaction and thus lessens the yield. It can be suppressed by adding some WCl_6 or some excess WOCl_4 into the reaction ampoule. The two different methods of synthesis show a distinct influence on the composition of the products. As indicated by EDX analyses and the results of the single crystal analyses, crystals obtained by method A show constantly a silver tungsten ratio of 1:2, indicating stoichiometric composition according to the formula $\text{Ag}[\text{W}_2\text{O}_2\text{Cl}_6]$. Crystals obtained by reaction B showed a variable silver tungsten ratio of 1:2, 0.66:2, 0.62:2 and 0.18:2, respectively, according to the site occupancy factors obtained by crystal structure determinations on crystals from different runs. The ratio 1:2, however, was only found in crystals obtained after opening the ampoules after the first reaction cycle, grinding the contents, re-sealing and heating for a second time, as described in the Experimental Part. The occurrence of such a large variety in the silver content is remarkable. The consequence for the charge balance of the crystal is the presence of a corresponding variety in the oxidation state of the tungsten atoms, ranging between +5 in $\text{WOCl}_3 = \text{W}_2\text{O}_2\text{Cl}_6$ and +4.5 in $(\text{Ag}^+)_{1.0}[\text{W}_2\text{O}_2\text{Cl}_6]$.

Crystal structure of $\text{Ag}_{1-x}[\text{W}_2\text{O}_2\text{Cl}_6]$

The crystal structures have been determined for several selected crystals and, for a crystal of the composition $\text{Ag}_{1.0}[\text{W}_2\text{O}_2\text{Cl}_6]$, at three different temperatures. All of these crystallize in the mono-

1
2
3 clinic space group $C2/m$ with structures isotypic to those of $Tl[W_2O_2Cl_6]$ or $K_{0.84}[W_2O_2Cl_6]$ [1]. The
4
5 basic building blocks are $^1_\infty[W_2O_2Cl_6]$ strands and Ag^+ ions coordinated by terminal Cl atoms of the
6
7 negatively charged $W_2O_{4/2}Cl_6$ groups (Fig. 1). The refined occupation factors of the Ag atoms re-
8
9 veal the large phase field width of the Ag content. The investigated crystals were found to have the
10
11 empiric formulae $Ag_{0.18}[W_2O_2Cl_6]$, $Ag_{0.62}[W_2O_2Cl_6]$ and $Ag_{1.0}[W_2O_2Cl_6]$, respectively. As a conse-
12
13 quence, the mean oxidation states of the W atoms span almost the complete region between +4.5
14
15 and +5, which has to be interpreted as a dynamically intervalent state since all W atoms occupy the
16
17 same crystallographic site $4i$. Neighbouring strands are bound together by Ag^+ ions to layers in the
18
19 $b-c$ plane (Fig. 2).

20
21 Refinement of anisotropic displacement parameters for Ag^+ ions on $(0, \frac{1}{2}, \frac{1}{2})$ resulted in an ex-
22
23 tremely elongated displacement ellipsoid and a high residual electron density. Splitting the position
24
25 of the Ag^+ ion over two closely neighbored sites $(0.048, \frac{1}{2}, 0.501)$ did not solve the problem:
26
27 though the residual electron density decreased clearly, no change in the elongation of the displace-
28
29 ment ellipsoids of the Ag^+ ions could be obtained. An electron density map in the (010) plane shows
30
31 a broad region of electron density smeared along $[100]$ with two closely neighbored maxima close
32
33 to the special position $2d$ ($2/m$) at $(0, \frac{1}{2}, \frac{1}{2})$. An alternative model for the refinement was set up,
34
35 implying four closely neighbored (symmetry generated seven) Ag sites using isotropic displace-
36
37 ment parameters. The actual electron density distribution was described better by this structure
38
39 model, even though strong correlations between parameters of the split Ag atoms occurred. To gain
40
41 further insight into the phenomenon data sets at low temperature were recorded. At 123 K the site
42
43 occupation factor of the 'central' Ag site in $(0, \frac{1}{2}, \frac{1}{2})$ became less than its error indicating a decreas-
44
45 ing electron density in the central point. So this site was set to 'not occupied' on refinements based
46
47 on the data collected at this temperature and the model contained six Ag sites (Fig. 1). The occupa-
48
49 tion factors were allowed for free refinement and finally reached a sum corresponding to the for-
50
51 mula $Ag_{1.02(6)}[W_2O_2Cl_6]$ (Tab. 2). In a third model, the electron density of the Ag ion was refined
52
53 using an anharmonic displacement model with the Gram-Charlier expansion of the harmonic dis-
54
55 placement tensor (program JANA2000 [13]). The Ag site was split into two symmetric equivalent
56
57 positions close to $(0, \frac{1}{2}, \frac{1}{2})$, each of them refined with a displacement tensor of 3rd order. The resid-
58
59 ual electron density decreased to an acceptable level but some correlations between parameters per-
60
sisted. Nonetheless it seems to be a method inherent phenomenon that parameters of the displace-
ment tensor are correlated [14]. Fig. 2 displays electron density charts of the Ag ion and a section
along the maxima of the electron density at 295 K, 193 K, and 123 K, and the shape of the anhar-

1
2
3 monic displacement parameters. At ambient temperature, the electron density of the Ag ion is
4 blurred over a distance of nearly 4 Å with two flat maxima, representing preferred positions for the
5 Ag ion. On decreasing temperature the two maxima of electron density persist but these maxima
6 become sharper and the distance between the maxima increases from 1.24(2) Å at 295 K to
7 1.473(8) Å at 123 K. The Ag ions are actually located in a double-minimum potential with a saddle
8 point of low energy. According to Boltzmann's distribution theorem $\frac{N_{E+\Delta E}}{N_E} = e^{\frac{-\Delta E}{kT}}$, the electron
9 density diagram can be transferred into a potential diagram assuming that the electron density repre-
10 sents the population of the respective position and the observed maximal electron density as the
11 population of the lowest energy state N_E . The result is shown at the bottom of Fig. 2 from which the
12 activation energy for the thermally activated hopping of the Ag⁺ ion between the two most preferen-
13 tial positions at 123 K is estimated to 10 meV or 1 kJ mol⁻¹. This fits with the thermal energy kT ,
14 which corresponds to 11 meV at 123 K.
15
16
17
18
19
20
21
22
23
24
25
26
27

28 In the crystal structure, the Ag⁺ ions exhibit a distorted bicapped cuboidal coordination environ-
29 ment. The coordination polyhedron consists of eight Cl(2) and Cl(3) atoms with cuboidal shape,
30 which is capped by two additional Cl(3) atoms (Fig. 1). This is caused by the lattice centering,
31 which shifts the planar W₂Cl₆ groups alternately by half of the lattice constant in the *b* direction and
32 brings two Cl(3) atoms of two neighbouring [W₂O₂Cl₆] strand in positions over two opposite faces
33 of the cuboidal void in the crystallographic *a* direction. Thus the migration paths of the Ag⁺ ions are
34 blocked and no long range ion mobility is possible since the structure of the anionic lattice does not
35 offer non-intermittent migration paths for ionic conduction and only a local mobility is observed.
36 The Ag–Cl distances amount 2.582(6) (Ag(4)–Cl(2)^{VII}), 2.653(6) (Ag(4)–Cl(3)), 2.976(6) Å
37 (Ag(4)–Cl(3)^{VI}) for the different Ag sites and are comparable for example with the Ag–Cl distances
38 in Ag₃YCl₆ (2.570 to 2.733 Å) [15]. Ag₃YCl₆ also contains disordered Ag ions with an elongated
39 electron density inside a pair of face sharing octahedra. A comparable situation is observed for one
40 of the Cu ions in the structure of tetrahedrite, Cu₁₂Sb₄S₁₃ [16]. The Cu ion is located in a trigonal
41 bipyramidal coordination environment with three S atoms in the equatorial plane and two antimony
42 atoms at the apexes. A dynamic disorder perpendicular to the triangular plane was observed by
43 temperature dependent structure determinations.
44
45
46
47
48
49
50
51
52
53
54
55
56
57

58 From the structure analyses of the silver deficient crystals the tendency is present that on decreasing
59 silver content an increasing W–W distance follows. With fully occupied silver sites in
60

1
2
3 $\text{Ag}_{1-x}[\text{W}_2\text{O}_2\text{Cl}_6]$, i.e. $x = 0$, a W–W distance of 2.8572(2) Å is found whereas for $x = 0.38$ this
4 distance amounts 2.8631(5) Å and for $x = 0.82$ it enlarges to 2.8949(4) Å. The decreasing Ag^+
5 content lowers the content of W(IV) with respect to W(V). The W–W distance thus enlarges to
6 reach finally the value found for WOCl_3 , containing only W(V) [1].
7
8
9

10 11 12 13 *Nuclear magnetic resonance analysis*

14
15
16
17 To gain further insight into the ionic motion process a nuclear resonance analysis was performed.
18 MAS-NMR measurements on ^{109}Ag nuclei were performed to obtain the isotropic chemical shift of
19 the silver ions. The MAS-NMR spectrum shows one signal at 232.0 ppm referenced to AgNO_3 (Fig.
20 3) This result is in accordance with the results of the X-ray single crystal structure analysis, which
21 showed the equivalence of the two minima of the double minimum potential. Further measurements
22 aimed on the longitudinal relaxation time T_1 . A sequence of pulses was used to make the magnetiza-
23 tion fade out. After a pulse delay (pd) a rectangular pulse was set to excite ^{109}Ag nuclei. The free
24 induction decay FID was plotted against pd . This procedure was performed at different tempera-
25 tures of 265, 300, 330 and 355 K. By using the *Bloch* equation [17] the spin lattice relaxation time
26 was calculated. The obtained relaxation times were plotted semi-logarithmic against the reciprocal
27 values of the corresponding temperatures (Fig. 3). By fitting a linear slope to the data points, the
28 Arrhenius equation can be applied and the activation energy of the Ag^+ ion motion thus be calcu-
29 lated. The Arrhenius plot showed a linear alignment following $\log T_1 = 0.6908 + 175.96 \text{ K} \cdot T^{-1}$. Ac-
30 cording to $\log T_1 = \log k_0 - \frac{E_A}{R} KT^{-1}$ the activation energy is calculated to 15.1 meV.
31
32
33
34
35
36
37
38
39
40
41
42
43
44

45 46 *Electrical Conductivity*

47
48
49 Like the others so far examined members of the $M_x[\text{W}_2\text{O}_2\text{Cl}_6]$ series, $\text{Ag}[\text{W}_2\text{O}_2\text{Cl}_6]$ is a good elec-
50 trical conductor. At room temperature, a specific conductivity of about $1 \text{ } \Omega^{-1} \text{ cm}^{-1}$ was found on a
51 pressed powder sample. The temperature characteristics is semi-conducting, since the conductivity
52 decreases with decreasing temperature and reaches about $10^{-3} \text{ } \Omega^{-1} \text{ cm}^{-1}$ at 25 K (Fig. 4).
53
54
55
56

57
58 From the Arrhenius equation for the activation energy of current transport in semiconductors one
59 gets $\sigma(T) = \sigma_0 \cdot e^{-\frac{\Delta E}{2kT}}$. Accordingly, $-\ln \sigma = f(T^{-1})$ is expected as a linear function. As Fig. 4 shows,
60

1
2
3 a linear function is actually present in the temperature range between 70 K and 300 K. From the
4 slope the energy of the thermal activation is calculated to 0.0298(1) eV. This corresponds to a band
5 gap of $\Delta E = 0.0596(2)$ eV. In the range below 70 K the activation energy decreases with decreasing
6 temperature and a linear function is no longer present. This behaviour may be interpreted with a
7 *variable range hopping* mechanism (*VRH*), describing the low temperature behaviour of the con-
8 ductivity in disordered solids. The temperature dependence of the conductivity follows the expres-
9 sion $\sigma(T) = \sigma_0 \cdot e^{-\left(\frac{T_0}{T}\right)^\alpha}$ [18]. Initially developed for amorphous solids, the model is nowadays used
10 also for crystalline semiconductors [19]. The exponent α is critical towards the dimensionality of
11 the process and is assumed to be 0.5 for 1D systems [20]. As can be seen from Fig. 4, a satisfying
12 fit to the conductivity data can be obtained with the exponent $\alpha = 0.53(2)$.
13
14
15
16
17
18
19
20
21
22
23
24
25

26 **Conclusion**

27
28
29 $\text{Ag}_{1-x}[\text{W}_2\text{O}_2\text{Cl}_6]$ represents a further member of the $A_{1-x}[\text{W}_2\text{O}_2X_6]$ family of compounds. A large
30 phase field width has been achieved for the Ag containing compound, ranging from full occupation
31 of the Ag^+ site down to an occupation of merely 18 %. The Ag^+ ions are mobile within their cuboi-
32 dal coordination sphere in a double minimum potential and are dynamically disordered with an ac-
33 tivation energy in the order of kT , shown by temperature dependent structure analyses and spin
34 lattice relaxation times based on ^{109}Ag solid state NMR spectra. The crystal structure, however,
35 does not allow for a long range mobility of the Ag^+ ions, since there are no continuous migration
36 paths for the Ag^+ ions. Like all other members of the $A_{1-x}[\text{W}_2\text{O}_2X_6]$ family of compounds,
37 $\text{Ag}[\text{W}_2\text{O}_2\text{Cl}_6]$ exhibits a remarkable high electrical conductivity with semiconducting characteristics
38 and a small band gap of approximately 60 meV.
39
40
41
42
43
44
45
46
47
48
49
50
51
52

53 **Acknowledgement**

54
55
56 We are much obliged to J. Daniels for measuring the X-ray diffraction data sets and to Prof. M.
57 Jansen, *Max-Planck-Institute for Solid State Research* in Stuttgart, Germany, for giving the oppor-
58 tunity for the conductivity measurements.
59
60

Table 1 Crystallographic data and details of the crystal structure determination of $\text{Ag}_{1.0}[\text{W}_2\text{O}_2\text{Cl}_6]$. The refinement is based on the model for the Ag electron density by 4 (295 K und 193 K) or 3 (123 K) closely neighboured sites. Ag atoms are refined with isotropic displacement parameters. The standard deviations in brackets refer to the last quoted digit.

Formula	Ag $[\text{W}_2\text{O}_2\text{Cl}_6]$		
Crystal system, space group	monoclinic, $C 2/m$		
Temperature of measurement / K	295(2)	193(3)	123(3)
Lattice parameters / Å	$a = 12.9211(3)$	$a = 12.8737(3)$	$a = 12.8499(6)$
	$b = 3.7631(1)$	$b = 3.7629(1)$	$b = 3.7626(2)$
	$c = 9.8663(3)$	$c = 9.8525(2)$	$c = 9.8477(5)$
	$\beta = 109.064(1)$	$\beta = 109.161(1)$	$\beta = 109.227(2)$
Cell volume / Å ³	453.42(2)	450.84(2)	449.57(4)
Number of formula units	2		
Calculated density / g cm ⁻³	5.276	5.306	5.321
Crystal size / mm ³	0.019 × 0.112 × 0.018		
Radiation	Mo-K α ($\lambda = 0.71073$ Å)		
Data collection range / °	$6.7 \leq 2\theta \leq 55.0$	$6.7 \leq 2\theta \leq 55.0$	$9.1 \leq 2\theta \leq 54.9$
min. / max. $h k l$	$-16 \leq h \leq 16$	$-16 \leq h \leq 16$	$-16 \leq h \leq 16$
	$-4 \leq k \leq 4$	$-4 \leq k \leq 4$	$-4 \leq k \leq 4$
	$-12 \leq l \leq 12$	$-12 \leq l \leq 12$	$-12 \leq l \leq 12$
Number of measured reflections	5736	5303	2395
Number of independent reflections	598	594	584
Data quality $R_{\text{int}}/R_{\text{sigma}}$	0.051 / 0.019	0.058 / 0.025	0.088 / 0.056
Number of refined parameters	46	46	44
Relation reflections / parameters	13.0	12.9	13.3
Absorption coefficient μ / cm ⁻¹	291.5	293.2	294.0
Min. / max. transmission	0.2599 / 0.7014	0.2561 / 0.7672	0.2857 / 0.7640
Quality of refinement			
$R(F)$	0.015	0.015	0.025
$R(F)$ ($n(F_o) > 4\sigma(F_o)$)	0.013 (566)	0.014 (577)	0.024 (562)
$wR(F^2)$	0.029	0.032	0.054
GooF	1.04	1.16	1.07
max./min. residual electron density [eÅ ⁻³]	+0.92 / -0.87	+0.89 / -0.84	+1.30 / -1.49

Table 2 Positional parameters and equivalent isotropic displacement factors U of the atoms in the structure of $\text{Ag}[\text{W}_2\text{O}_2\text{Cl}_6]$ at 123 K. Values in brackets are standard deviations referring to the last quoted digit. All atoms are located on Wyckoff site $4i$ with site symmetry m . SOF is the respective site occupation factor for the split positions of the Ag atom. The sum of the occupation factors amounts $\sum \text{SOF}_{2\text{Ag}(2)+2\text{Ag}(3)+2\text{Ag}(4)} = 1.02(6)$

Atom	SOF	x	y	z	$U_{\text{eq}}/\text{\AA}^2$
W		0.01132(3)	0	0.14890(3)	0.00698(18)
O		0.0096(5)	$\frac{1}{2}$	0.1466(5)	0.0085(13)
Cl(1)		0.15815(18)	0	0.0503(2)	0.0101(4)
Cl(2)		0.15555(18)	0	0.3716(2)	0.0141(5)
Cl(3)		-0.10774(19)	0	0.2928(2)	0.0151(4)
Ag(2)	0.13(2)	0.023(3)	$\frac{1}{2}$	0.4962(11)	0.016(2)
Ag(3)	0.265(17)	0.058(2)	$\frac{1}{2}$	0.5025(8)	0.0131(15)
Ag(4)	0.114(13)	0.099(2)	$\frac{1}{2}$	0.5240(15)	0.016(3)

1
2
3
4
5
6
7
8
9
10
11
12
13
14
15
16
17
18
19
20
21
22
23
24
25
26
27
28
29
30
31
32
33
34
35
36
37
38
39
40
41
42
43
44
45
46
47
48
49
50
51
52
53
54
55
56
57
58
59
60

References

- [1] J. Beck, Ch. Kusterer, R.-D. Hoffmann, R. Pöttgen, *J. Solid State Chem.* **2006**, *179*, 2298-2309.
- [2] J. Beck, Ch. Kusterer, *Z. Anorg. Allg. Chem.* **2008**, *634*, 587-592.
- [3] Y.-Q. Zheng, K. Peters, H.G. v. Schnering, *Z. Anorg. Allg. Chem.* **1998**, *624*, 1415-1418.
- [4] S. Imhaïne, C. Perrin, M. Sergent, *Mat. Res. Bull.* **33** (1998) 927-933.
- [5] P. Zönnchen, G. Thiele, C. Hess, C. Schlenker, H. Bengel, H.-J. Cantow, S.N. Magonov, D.-K. Seo, M.-H. Whangbo, *New J. Chem.* **1996**, *20*, 295-300.
- [6] H. Hillebrecht, P. J. Schmidt, H. W. Rotter, G. Thiele, P. Zönnchen, H. Bengel, H.-J. Cantow, S. N. Magonov, M.-H. Whangbo, *J. Alloys Comp.* **1997**, *246*, 70-79.
- [7] P. Würfel, H. D. Hausen, K. Krogmann, P. Stampel, *Phys. Stat. Sol.(A)* **1972**, *10*, 537-541.
- [8] H.-J. Lunk, W. Petke, *Z. Chem.* **1974**, *14*, 365.
- [9] R. Colton, I. B. Tomkins, *Austral. J. Chem.* **1965**, *18*, 447 - 452.
- [10] W. Herrendorf, H. Bärnighausen, *HABITUS, Program for the Numerical Absorption Correction*, Universities of Karlsruhe and Gießen, Germany, 1993,1997.
- [11] G. M. Sheldrick, *SHELX97 [includes SHELXS97, SHELXL97, CIFTAB] - Programs for Crystal Structure Analysis (Release 97-2)*. University of Göttingen, Germany, **1998**.
- [12] L. J. Farrugia, *J. Appl. Cryst.* **1999**, *32*, 837-838.
- [13] V. Petricek, M. Dusek, L. Palatinus, *Jana2000 - The crystallographic computing system*, Institute of Physics, Praha, Czech Republic, **2000**.

- 1
2
3 [14] B. Bagautdinov, J. Luedecke, M. Schneider, S. van Smaalen, *Acta Crystallogr. B* **1998**, *54*,
4 626-634.
5
6
7
8
9 [15] K. Lerch, W. Laqua, G. Meyer, *Z. Anorg. Allg. Chem.* **1990**, *582*, 143-150.
10
11
12 [16] A. Pfitzner, M. Evain, V. Petricek, *Acta Crystallogr.* **1997**, *B53*, 337-345.
13
14
15
16 [17] H. W. Spieß, R. Groseescu, U. Haeberlen, *Chem. Phys.* **1974**, *6*, 226-234.
17
18
19 [18] N. F. Mott, E. A. Davis, *Electronic Processes in Non-Crystalline Solids*, Oxford University
20 Press, London, 1971.
21
22
23
24 [19] Ch. Büscher, U. Stöhr, W. Freyland, *Phys. Chem. Chem. Phys.* **2000**, *2*, 2261-2264; R. Pocha,
25 D. Johrendt, B. Ni, M. M. Abd-Elmeguid, *J. Amer. Chem. Soc.* **2005**, *127*, 8732-8740; E.
26 Arushanov, S. Siebentritt, T. Schedel-Niedrig, M. Ch. Lux-Steiner, *J. Appl. Phys.* **2006**, *100*,
27 063715.
28
29
30
31
32
33 [20] P. A. Lee, *Phys. Rev. Lett.* **1984**, *53*, 2042-2045; M. M. Fogler, S. Teber, B. I. Shkloskii, *Phys.*
34 *Rev.* **2004**, *69B*, 035413/1-18.
35
36
37
38
39
40
41
42
43
44
45
46
47
48
49
50
51
52
53
54
55
56
57
58
59
60

Legends for Figures

Fig. 1 Section of the chain of edge sharing pairs of $[\text{WO}_{2/2}\text{Cl}_2\text{Cl}_{2/2}]$ octahedra in the structure of $\text{Ag}_{1.0}[\text{W}_2\text{O}_2\text{Cl}_6]$ at 123 K (top), the unit cell of $\text{Ag}_{1.0}[\text{W}_2\text{O}_2\text{Cl}_6]$ in a view along the crystallographic b axis (middle, the Ag ions are represented by their harmonic displacement components U_{ij}), and the coordination of the dynamically disordered Ag ion by surrounding Cl atoms (bottom, the Ag ions are represented by their isotropic displacement components U). The displacement spheres and ellipsoids comply with a probability of localization of 90 %. Bond lengths /Å and angles / ° at 123 K: $\text{W}-\text{W}^{\text{I}}$ 2.8501(4), $\text{W}-\text{O}$, $\text{W}-\text{O}^{\text{II}}$ 1.8815(1), $\text{W}-\text{Cl}(1)$ 2.390(2), $\text{W}-\text{Cl}(1)^{\text{I}}$ 2.403(2), $\text{W}-\text{Cl}(2)$ 2.404(2), $\text{W}-\text{Cl}(3)$ 2.360(2), $\text{O}-\text{W}-\text{O}^{\text{II}}$ 178.5(4), $\text{Cl}(1)-\text{W}-\text{Cl}(1)^{\text{I}}$ 107.03(6), $\text{Cl}(2)-\text{W}-\text{Cl}(3)$ 84.83(7), $\text{W}-\text{Cl}(1)-\text{W}^{\text{I}}$ 72.97(6). Symmetry generated atoms are marked by superscript indices : I = $-x, y, -z$; II = $x, -1+y, z$; III = $-x, y, 1-z$; IV = $x, y, 1-z$; V = $x, 1+y, z$; VI = $\frac{1}{2}-x, \frac{1}{2}+y, 1-z$; VII = $-x, 1+y, 1-z$.

Fig. 2 Representation of the electron density of the Ag ion in the structure of $\text{Ag}_{1.0}[\text{W}_2\text{O}_2\text{Cl}_6]$ (left, based on Fourier coefficients F_{O} , axis labellings refer to crystal coordinates, contour lines are graded by $2 e/\text{Å}^3$), sections of the electron density function through the maxima parallel to the crystallographic c axis (middle) and representations of the anharmonic displacements of the Ag atoms, drawn to include a probability density of 70 % (right). On bottom the respective double-minimum potential function for the Ag ion at 140 K is shown.

Fig. 3 ^{109}Ag MAS NMR spectrum of $\text{Ag}_{1.0}[\text{W}_2\text{O}_2\text{Cl}_6]$, recorded with a rotation frequency of 10 kHz (top) and the function of the spin lattice relaxation time at different temperatures versus the reciprocal temperature including the corresponding linear regression function (bottom).

Fig. 4 Electrical conductivity of a compressed sample of $\text{Ag}_{1.0}[\text{W}_2\text{O}_2\text{Cl}_6]$ as a function of temperature. The conductivity is shown on a logarithmic scale (top) and the respective Arrhenius function $-\ln \sigma = f(T^{-1})$ (bottom). Two different functions have been fitted to the data, a linear fit for the high temperature region (a) and a fit according the VRH model (b).

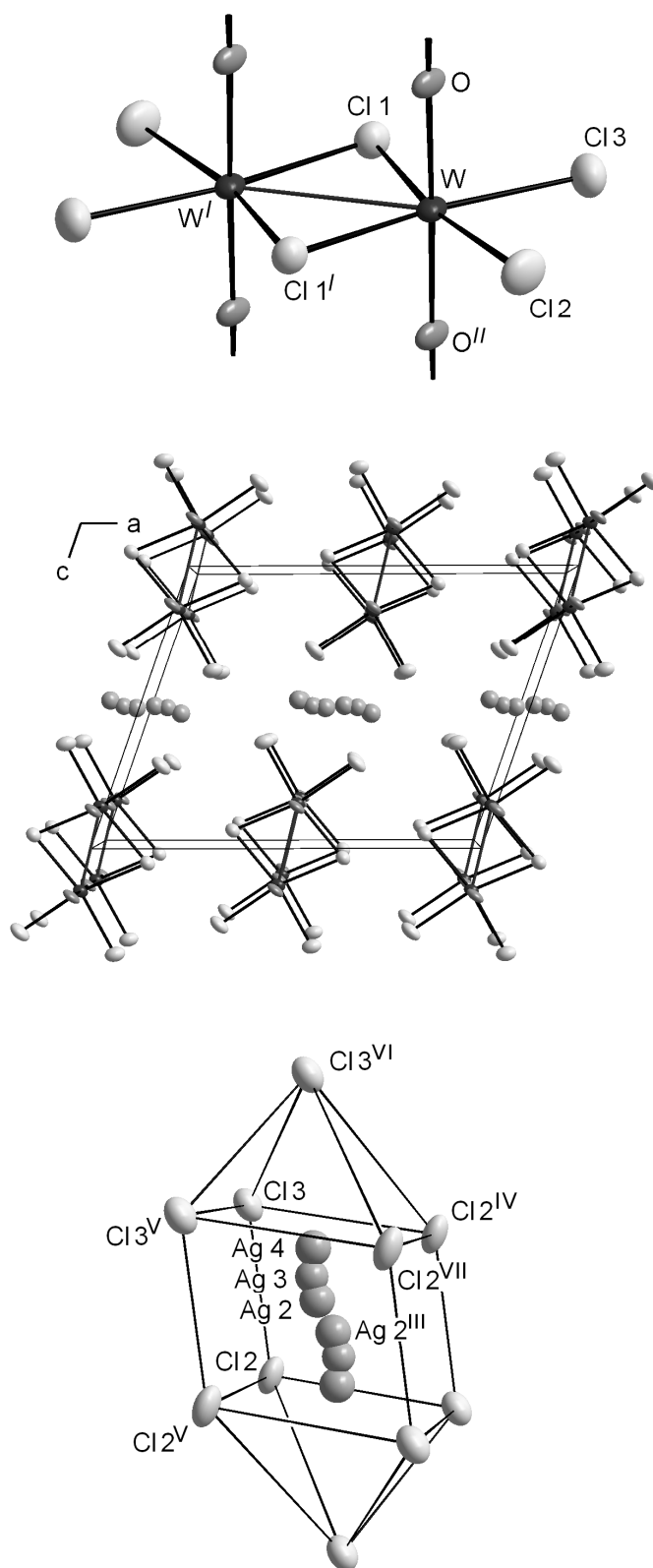


Fig. 1

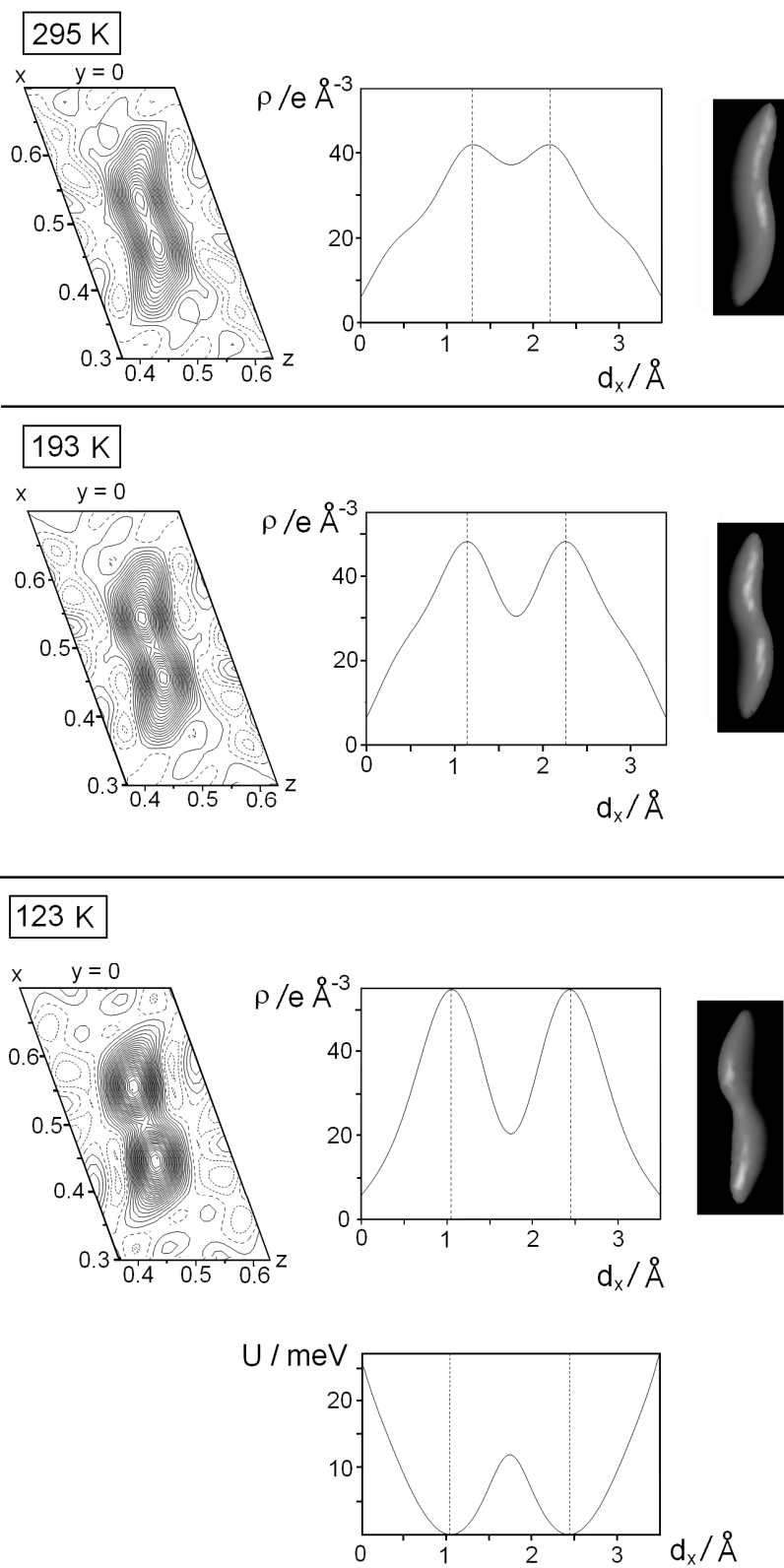


Fig. 2

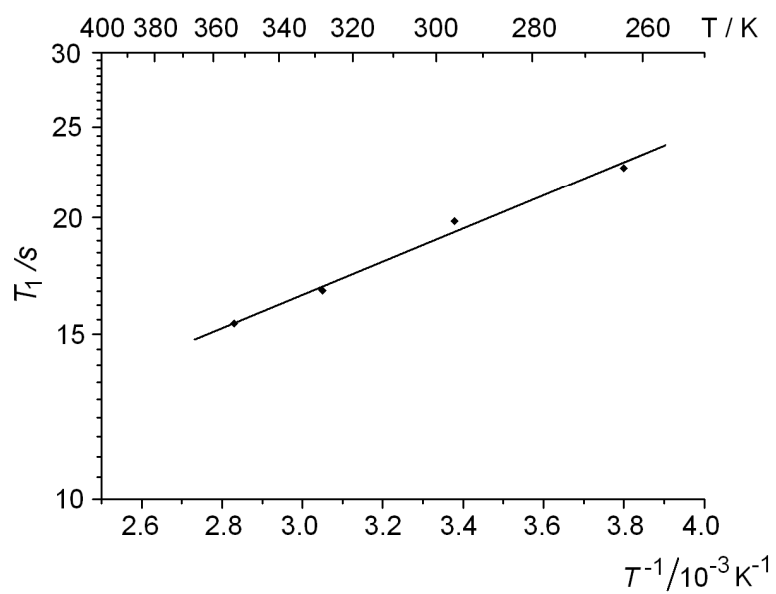
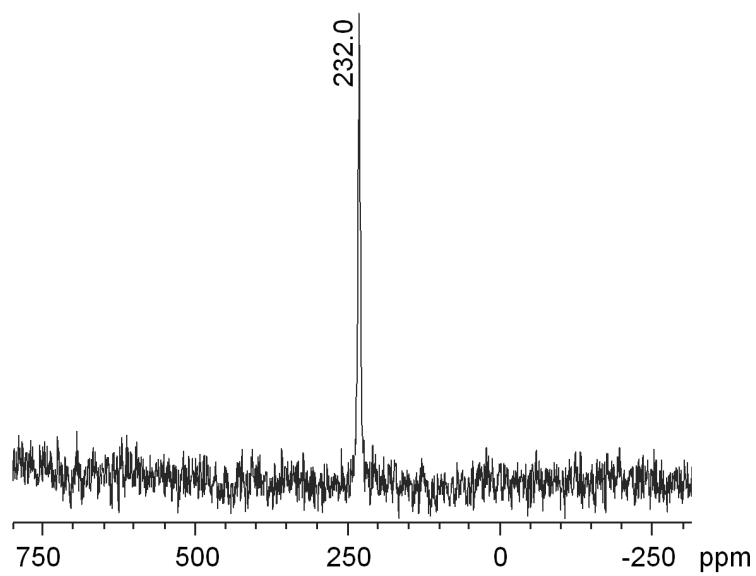


Fig. 3

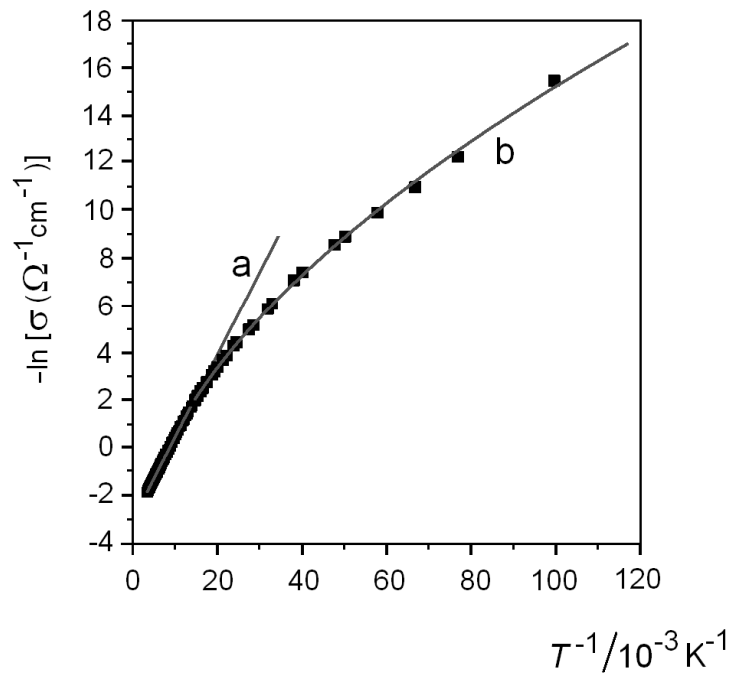
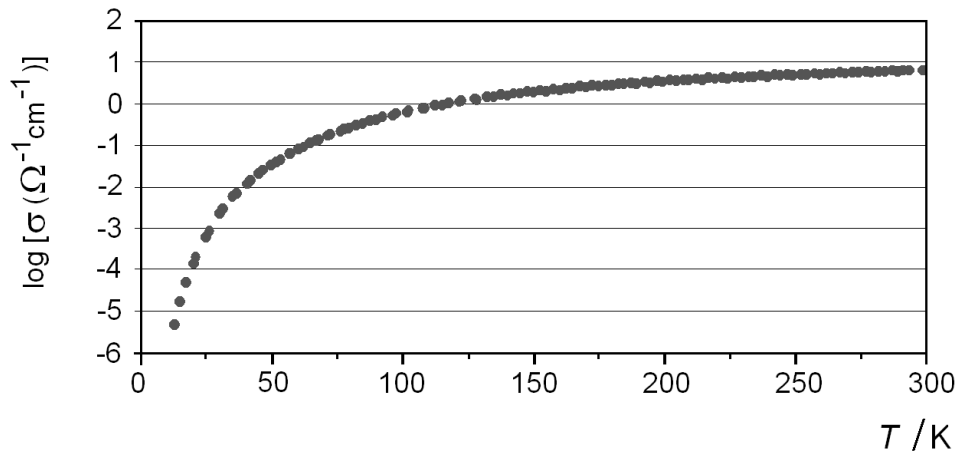


Fig. 4